

Luminosity enhancement by a self-ionized plasma in e^+e^- collisions

P. Chen and C.-K. Ng

Stanford Linear Accelerator Center, Stanford University, Stanford, California 94309

S. Rajagopalan

Physics Department, University of California, Los Angeles, Los Angeles, California 90024

(Received 21 January 1993)

We employ a two-dimensional particle-in-cell code to investigate the focusing of relativistic charged-particle beams in plasmas. The intense electric fields generated by electron and positron beams in high-energy physics experiments can ionize a gas into a plasma which will then focus the beams. The self-ionization mechanism will enhance the luminosity in e^+e^- collisions by implementing a plasma lens in the interaction region. We investigate the dependences of the luminosity enhancement on the plasma lens thickness and plasma density. The application of plasma lens focusing to the Stanford Linear Collider is discussed.

PACS number(s): 41.75.Fr, 52.40.Mj, 52.70.-m

I. INTRODUCTION

Achieving high enough luminosities (event rates) for physics studies is one of the important goals for e^+e^- linear colliders. The Stanford Linear Collider (SLC) is the first linear collider to study the fundamental electroweak gauge particle Z by colliding electron and positron beams at ~ 92 GeV center-of-mass energy. Small spot sizes ($\sim 1-2 \mu\text{m}$) can be obtained by the final focusing optics at SLC. Plasma focusing can in principle provide a mechanism by which to pinch the beams to even smaller size before they collide at the interaction point.

The self-focusing plasma lens has been proposed as a mechanism to increase the luminosity in e^+e^- linear colliders [1]. Conventional quadrupole magnets for final on-line focusing in high-energy accelerators have limited focusing strength (a few hundred MG/cm), while plasma lenses are able to produce focusing strength a few orders of magnitude higher, depending on the plasma density. This self-focusing effect by the plasma on relativistic beams has been verified experimentally at the Argonne National Laboratory [2] and Japan [3].

Since the introduction of the self-focusing plasma lens, the study of plasma focusing has been divided into the overdense regime [4] (i.e., the beam peak density n_b is much smaller than the ambient plasma density n_p) and the underdense regime [5,6] ($n_b > n_p$). In the overdense regime, the beam quantities can be treated as perturbations. Hence, the plasma dynamics can be well described by linear fluid theory. Although the focusing is strong in this regime, the beam optics are subject to aberrations due to the spatial dependence of the focusing strength. Furthermore, the high plasma density may pose backgrounds to particle detectors. In the underdense regime, the focusing strength for electron beams is more uniform, and that for positron beams becomes nonlinear.

Recently, it has been proposed that considerable luminosity gain can be achieved by using the beams themselves to ionize a gas into a plasma, which subsequently

focuses the beams [7]. The major mechanism is tunneling ionization, a consequence of the distortion of the atomic potential by the strong electric field carried by the intense, charged-particle beam. This self-ionization mechanism provides an attractive means by which to implement a plasma lens for final focusing in e^+e^- collisions, as it is nontrivial to produce high density plasmas at the center of a complex detector.

Previous studies [1,7] have neglected the effects of the ion motion in the plasma. Because of the strong field exerted by the beams, the ions are expected to move to neutralize the space charge forces of the beams. On the other hand, the self-ionization process mentioned above is determined spatially by the beam fields, which have to be solved self-consistently when the beams collide. In view of this, simulations are required to accurately account for the complicated dynamics of beam-plasma interactions.

The purpose of this work is to simulate beam plasma interactions by the self-ionization mechanism and to investigate the maximum attainable enhancement of luminosity. We will use SLC beams as an example. Our main objective is to determine the plasma density and plasma lens thickness for maximum luminosity enhancement at SLC. This paper is organized as follows. In the next section, the basic principles of plasma lens focusing are briefly reviewed. In Sec. III, the self-ionization mechanism of an intense, charged-particle beam is discussed. In Sec. IV, we employ the two-dimensional (2D) particle-in-cell electromagnetic code CONDOR [8], to simulate beam-plasma interactions and to study the phenomenon of self-focusing. The dependences of the luminosity enhancement on the plasma density and plasma lens thickness at SLC are also investigated. Section V contains discussions and a summary of results.

II. PLASMA FOCUSING OF BEAMS

The theory and the literature have thus far [4-6] separated focusing by plasmas of density greater than the beam (overdense lens) and by those of lesser density (un-

derdense lens). This distinction, for the purpose of analysis, nevertheless may obscure the unifying features of plasma focusing. We will attempt a description of beam-plasma interaction which describes the focusing aspect of the plasma response. The beams themselves are ultrarelativistic, and thus the intrabeam forces are compensated by a factor of $1/\gamma^2$, when propagating in a vacuum. When the beam impinges a plasma, the initial response of the plasma is to neutralize the electric field of the beam, not necessarily completely. As a consequence, the beam particles always experience a net force (intra-beam forces being almost fully balanced) which focuses them, due to ions for e^- beams and excess electrons for e^+ beams. The magnetic response of the plasma occurs in a much slower fashion and for our purposes is only a correction. The difference between an overdense and an underdense lens for an electron beam is mainly in the optical properties of the lens. In the case of an overdense lens, the frequency of oscillation of the plasma electrons is high, and the focusing strength follows the beam longitudinal profile with an oscillatory term due to the plasma electron oscillation. For underdense lenses, the plasma oscillation has a smaller frequency, and in our examples the beam has a length smaller than the plasma wavelength. This results in the expulsion of plasma electrons from the beam interior and the beam being focused by the plasma ions. For e^+ beams the overdense scenario is similar to the e^- case, but, for underdense lenses, the plasma electrons oscillate in the field of the beam and provide a focusing force while in the beam interior.

In general, the β function of the beam focusing in a plasma is governed by the third-order differential equation:

$$\beta''' + 4K\beta' + 2K'\beta = 0, \quad (1)$$

where $K = K(s)$ is the focusing strength and is, in general, a function of the longitudinal position of the beam. Let the plasma density be determined by the initial beam density with a ratio η as

$$n_p = \eta n_{b0}. \quad (2)$$

Note that η is also a function of beam position. Assuming a cylindrically symmetric bi-Gaussian beam-density profile $\rho_b = n_b e^{-r^2/2\sigma_r^2} e^{-z^2/2\sigma_z^2}$, the peak beam density is then $n_b = N/(2\pi)^{3/2} \sigma_r^2 \sigma_z$. In terms of the initial beam size $\sigma_{r0}^2 = \beta_0 \epsilon_n \gamma^{-1}$ we can write

$$K = \frac{\eta N r_e}{\sqrt{2\pi} \beta_0 \epsilon_n \sigma_z} \equiv \frac{\eta \zeta}{\beta_0}, \quad (3)$$

where ϵ_n is the normalized emittance. Here, we also introduce the phase-space density ζ , which measures beam density in the three-dimensional beam volume of r, r', z .

A. Focusing by an underdense lens

Assuming that the ions are infinitely heavy, an underdense plasma reacts to an electron beam by total rarefaction of the plasma electrons inside the beam volume, producing a uniform ion column of charge density en_p . This uniform column produces linear, nearly aberration-free

focusing. Simulations have shown that $n_b \sim 2n_p$ is needed to produce linear focusing over most of the bunch [6].

In the underdense plasma regime, the focusing strength K is determined by the density of the plasma, and is essentially constant inside the bulk plasma:

$$K = 2\pi r_e n_p / \gamma. \quad (4)$$

In practice we will choose $\eta \sim \frac{1}{2}$ in Eq. (3) to ensure the underdense condition. To solve Eq. (1), we first integrate the δ function in K' at the start of the lens, and obtain $\Delta\beta'' = -2K\beta_0$. The other two initial conditions are the continuity requirements $\beta' = \beta'_0$ and $\beta = \beta_0$. Also note that $\beta'_0 = 2/\beta_0^*$ just before the lens, where β_0^* is the value at the waist that would be formed in the absence of the lens. The equation of motion is then $\beta'' + 4K\beta = 2/\beta_0^* + 2\zeta$, and we obtain [5]

$$\beta = \frac{\beta_0}{2} + \frac{1}{2K\beta_0^*} + \left[\frac{\beta_0}{2} - \frac{1}{2K\beta_0^*} \right] \cos[\nu(s - s_0)] + \frac{2s_0}{\nu\beta_0^*} \sin[\nu(s - s_0)], \quad (5)$$

where $\nu = 2\sqrt{K}$. This solution demonstrates oscillatory behavior without damping effects. We further assume that $\beta_0 = \beta_0^*$ and $s_0 = 0$. To minimize backgrounds, we look for the next waist at $\sin(\nu s^*) = 0$. The path length is then

$$s^* = \frac{\pi}{\nu} = \frac{\pi}{2\sqrt{K}}. \quad (6)$$

The corresponding β^* is

$$\beta^* = \frac{1}{K\beta_0^*} = \frac{1}{\eta\zeta}. \quad (7)$$

To illustrate this result, we note that beam parameters $N = 4.0 \times 10^{10}$, $\sigma_z = 0.2$ mm, normalized emittance $\epsilon_n = 4 \times 10^{-3}$ cm, and $\beta_0^* = 1$ cm give $\zeta = 56$ cm $^{-1}$. If $\eta = 0.5$ is assumed, this will give $\beta_-^* = 0.36$ mm, which is a factor of ~ 28 reduction in β^* , or about a factor of 5 reduction in beam spot size. The corresponding path length is $s_-^* \simeq 2.10$ mm.

For an underdense plasma interacting with a positron beam, the plasma electrons are drawn toward the beam axis by the focusing potential provided by the positron beam. This results in a simultaneous motion of these electrons which is oscillatory and moving with the beam. In each cycle of oscillation the plasma electrons spend a fractional amount of time inside the core of the positron beam, resulting in an effective concentration of negative charge that provides a focusing force. Since the focusing force is nonlinear, the net effect is not simple to describe analytically.

B. Focusing by an overdense lens

From Ref. [1] the focusing strength of an overdense lens (where the plasma response can be treated as a perturbation) at the middle of a Gaussian bunch is

$$K = \frac{r_e N}{(2\pi)^{1/2} \gamma \sigma_r^2 \sigma_z} . \quad (8)$$

In a thick lens where the beam size continues to change,

$$K(s) = \frac{2\pi r_e n_b}{\gamma} = \frac{\xi}{\beta(s)} . \quad (9)$$

Inserting Eq. (9) into Eq. (7), we have

$$\beta''' + \frac{2\xi\beta'}{\beta} = 0 . \quad (10)$$

Integrating twice, the second time after multiplication by β' , one finds

$$\frac{\beta'}{2} = \frac{\beta - \beta_0^*}{\beta_0^*} + \xi\beta \ln(\beta_0^*/\beta) . \quad (11)$$

The exact solution to this nonlinear equation is nontrivial. Notice, however, that the very purpose of a plasma lens is to reduce β^* . Thus by definition $b \equiv \beta^*/\beta_0^* \ll 1$, and the term β/β^* on the right-hand side can be neglected in a perturbative approximation. Then the solution is

$$b_0^b = \exp\{-1/\xi\beta_0^*\} . \quad (12)$$

When restoring the β/β_0^* in Eq. (11) by the value of b_0 , we find an improved solution

$$b_1^b = \exp\{-(1-b_0)/\xi\beta_0^*\} . \quad (13)$$

This iterative process can continue to the degree of accuracy that one desires.

III. IONIZATION PROCESSES [7]

There are essentially two ionization mechanisms that can be provided by a high intensity, high-energy beam, namely, the collisional ionization and the tunneling ionization. In the following, we discuss in detail the relative importance of these ionization processes.

A. Collisional ionization

Collisional ionization is an ionization process in which an individual beam particle ionizes an atom by a virtual photon exchange. The cross section can be estimated via the photoionization cross section, using the Weiszacker-Williams spectrum. The ionization cross section in the equivalent photon approximation is given by [9]

$$\sigma_i = \frac{\alpha}{2\pi} \int_{\omega_1}^E \left[\ln \left[\frac{2E^2}{m\omega} \right] - 1 \right] \frac{\sigma_\gamma(\omega)}{\omega} d\omega + \frac{2\pi\alpha^2 Z}{m\omega_1} , \quad (14)$$

where

$$\frac{1}{\omega_I} = \frac{1}{Z} \sum_{n=1}^Z \frac{1}{\omega_n} .$$

For hydrogen atoms, $Z=1$ and $\omega_I = \omega_1 = 13.6$ eV. The spectrum $\sigma_\gamma(\omega)$ can be parametrized from photoionization data as

$$\sigma_\gamma(\omega) \approx \left[\frac{27}{\omega \text{ (eV)}} \right]^3 \text{ Mb} . \quad (15)$$

For SLC beams, $E=45$ GeV and we find $\sigma_i \sim 0.22$ Mb. The fraction of atoms that can be ionized through this mechanism by an incoming beam with N particles and size σ_r is $R_i = N\sigma_i/4\pi\sigma_r^2$. For SLC beams, $\sigma_r \sim 1 \mu\text{m}$ and $N \sim 10^{10}$, so R_i is only on the order of a few percent, which is far from saturation. One therefore needs to have a gas which is $1/R_i$ times denser to provide the necessary amount of plasma. This is not desirable, however, as the backgrounds become very large. In addition, the nonsaturation of ionization also causes the tail of the beam to encounter a higher concentration of plasma than the head of the beam. This results in different foci for parts of the beam from different longitudinal positions. In this paper, therefore, we neglect collisional ionization in our self-ionization process.

B. Tunneling ionization

There is another ionization mechanism which relies on the collective field of the beam. When an external electric field is strong enough that the atomic Coulomb potential is sufficiently distorted, there is a finite probability that the bound state electron can tunnel through the potential barrier and become free. For hydrogen atoms, the ionization probability (per unit time) is given by [10]

$$W = 4 \frac{\alpha^5 c}{\chi_c^2} \frac{mc^2}{eE} \exp \left\{ -\frac{2}{3} \frac{\alpha^3}{\chi_c} \frac{mc^2}{eE} \right\} , \quad (16)$$

where E is the external electric field. The coefficient in the exponent is $\frac{2}{3}(\alpha^3/\chi_c)(mc^2/eE) \approx 34.1$ eV/Å. It is interesting to note that the ionization probability is already substantial long before the exponent reaches a value of the order unity due to the typical largeness of the nonexponential part. For example, an external field of 3.41 eV/Å would give $W \approx 1.15 \times 10^{14} \text{ sec}^{-1}$. Under this condition, the ionization will be saturated within 10 fsec. In fact, it can be shown for a field strength larger than $eE_{\text{th}} = 3.72$ eV/Å, where the ground-state binding energy is above the potential barrier, that, even classically, the electron can escape from the atom. The maximum collective electric-field strength in a bi-Gaussian beam can be calculated to be $eE_{\text{max}}/mc^2 \approx r_e N/2\sigma_z \sigma_r$, where r_e is the classical electron radius. A maximum field strength of 3.72 eV/Å corresponds to, for example, a beam of $N = 2.12 \times 10^{10}$, $\sigma_z = 0.2$ m, and $\sigma_r = 2.0 \mu\text{m}$. This is within the range of the SLC parameters.

In our scheme, both the tunneling ionization and the plasma response rely on the same field strength in the beam, yet the two effects in principle may act against each other. The very nature of the plasma response is to neutralize the space-charge field due to the beam [1]. If the charge neutralization is complete, as in the case of an overdense plasma lens, within a time scale which is comparable to that for the tunneling ionization process, then the beam field would be effectively screened off before the ionization can be saturated. For an underdense plasma lens the plasma response can never completely neutralize the space charge, and the problem is less severe. To ensure that our scheme indeed works, let us insist that the time scale involved in the ionization process τ_i be much

less than the time scale of plasma response to the beam field τ_p , which in turn should be much less than the beam passage time τ_b : $\tau_i \ll \tau_p \ll \tau_b$. The last inequality is the known condition for the plasma lens. The first condition $\tau_i \ll \tau_p$ ensures that the ionization saturates before charge neutralization is effective.

Saturation of tunneling ionization by an incoming beam occurs when the integrated ionization probability is close to unity. The function $W(z)$ is an extremely rapid function of z and thus the position z_s where the probability becomes almost unity is not different from the position where the integrated rate is one. Therefore it is reasonable to use the relation

$$1 = \int_{-\infty}^{z_s} W(z) dz / c, \quad (17)$$

where z_s is the position along the beam where the ionization is saturated. Since $W(z)$ is exponentially dependent on $E(z)^{-1}$ of the beam, while $E(z)$ itself follows a Gaussian distribution, we expect that the saturation is predominantly in the small time interval. For example, $\tau_i \sim W^{-1}(z_s)$ fsec around the saturation point z_s . On the other hand, as we will see in the following, the underdense plasma density matched to the SLC-like beam density is of the order of $n_p \sim 10^{18} \text{ cm}^{-3}$, which corresponds to a plasma frequency of $\omega_p \sim 5.6 \times 10^{13} \text{ sec}^{-1}$. The typical time scale of plasma perturbation is therefore $\tau_p \sim 2\pi\omega_p^{-1} \sim 100$ fsec, which is longer than the time scale of tunneling ionization, yet shorter than the beam passage time $\tau_b \sim 1000$ fsec. Thus for the beam conditions we anticipate, the three time scales follow the right ordering.

IV. NUMERICAL RESULTS

To give a quantitative account of beam-plasma interactions, we employ the $2\frac{1}{2}$ -D particle-in-cell code CONDOR [8] to simulate the propagation of relativistic electron and positron beams in plasmas. CONDOR is a $2\frac{1}{2}$ -D, fully electromagnetic particle-in-cell code in which the dynamics of plasma and beam particles are treated self-consistently by the Maxwell equations and the Lorentz force equations. In order to calculate the luminosity enhancement by self-ionization, we have modified CONDOR to include a luminosity calculation and an algorithm for the ionization of gases triggered by the strong electric fields of relativistic charged-particle beams.

A. Beam focusing in plasmas

The geometry of our simulations is in r - z coordinates. Hence, the beams and the plasma are taken to be cylindrically symmetric. The electron and positron beams are injected from the boundaries in the $+\hat{z}$ and $-\hat{z}$ directions, respectively. To demonstrate the phenomenon of self-pinching of relativistic beams in plasmas, a preformed plasma is assumed in this subsection. The details of self-focusing effects due to tunneling ionization and its effect on luminosity enhancement will be examined in a later subsection.

The density profile for a cylindrically symmetric bi-

Gaussian beam is

$$\rho_b = n_b e^{-r^2/2\sigma_r^2} e^{-z^2/2\sigma_z^2}, \quad (18)$$

where the peak beam density n_b is related to the number of particles N in the bunch as

$$n_b = N / (2\pi)^{3/2} \sigma_r^2 \sigma_z. \quad (19)$$

To simulate the SLC beams, we take $N = 4 \times 10^{10}$, $\sigma_z = 0.2 \text{ mm}$, and $\sigma_r = 2 \text{ }\mu\text{m}$. The corresponding peak beam density $n_b = 3.17 \times 10^{18} \text{ cm}^{-3}$.

We are interested in determining the plasma lens density and thickness for maximum gain of luminosity in e^+e^- collisions, as will be discussed later. Thus, we initially choose $n_p = 3 \times 10^{18} \text{ cm}^{-3}$ for the plasma density. The simulations run from plasmas which are underdense to overdense plasmas.

The initial conditions for our simulation are as follows. The energies of the electron and positron beams are taken to be 45 GeV which has been achieved at SLC. The emittance of the beams is $4 \times 10^{-10} \text{ mrad}$ and the corresponding $\beta^* = 10 \text{ mm}$ (contrast with 5 mm as the design goal) in the final focusing region before the beams enter the plasma lens. The plasma electrons and ions are assumed to be stationary initially, and the plasma lens has a thickness of 4 mm.

In Fig. 1 we show the results from a CONDOR run for the behaviors of the e^+ and e^- beams as they traverse and collide in a preformed plasma. The plasma fills the whole region of each figure initially. The electrons are injected from the left boundary and the positrons from the

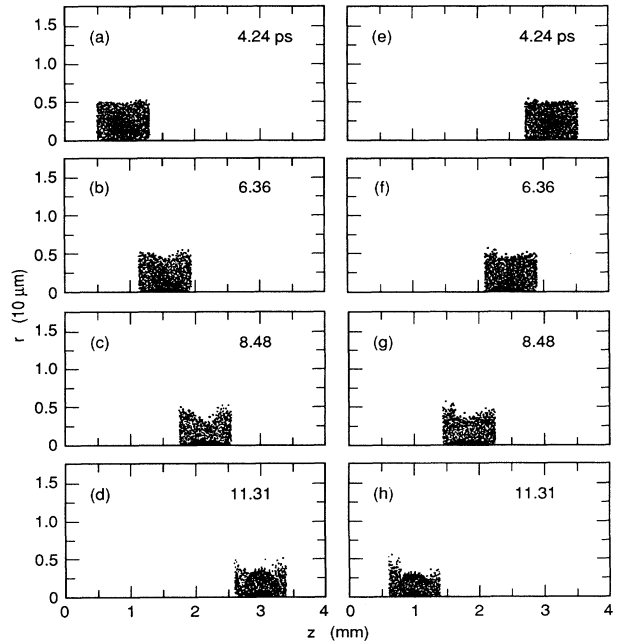


FIG. 1. Collision of e^+ and e^- beams in a preformed plasma. (a)–(d) for four different snapshots at 4.24, 6.36, 8.48, and 11.31 psec, respectively, for the e^- beam; (e)–(h) are for the corresponding e^+ beam.

right, and for clarity they are shown separately. Figures 1(a)–1(d) and 1(e)–1(h) are snapshots at four different time steps for the distributions of the e^- and e^+ beams, respectively. From Figs. 1(a)–1(b) and 1(e)–1(f), it can be seen that the electrons and positrons are focused by the plasma before they collide near the middle of the lens. The beam fronts are not focused well compared with the cores, as the plasma electrons are still responding to the relatively weaker field associated with the Gaussian nature of the beams. Near the center of the bunch, the stronger electromagnetic fields of the e^- and e^+ beams cause the plasma electrons to respond with greater amplitude and hence the focusing is stronger. For a highly relativistic charged-particle beam traveling in a vacuum, the self-pinching due to the magnetic field generated by the beam current is almost balanced by the repulsive space-charge force. However, in a plasma, we clearly see that the beams are pinched as a result of the neutralization of the space-charge forces of the beams by the plasma electrons or ions. In Figs. 1(c) and 1(g), the beams collide after they have been focused by the plasma to smaller effective sizes near the axis. It can also be seen that the outer cores of the beams are not focused as well as the central parts. This is due to the fact that the beam density in the outer region is smaller than the plasma density, and is a characteristic of beam focusing in an overdense plasma [see Eq. (8)]. Note that the peak beam density $3.17 \times 10^{18} \text{ cm}^{-3}$ at the center is about the same as the ambient plasma density $3 \times 10^{18} \text{ cm}^{-3}$. In Figs. 1(d) and 1(h), the two beams start to diverge again after colliding, and this completes the process of e^+e^- collision in the plasma. It is important that the beams collide at their focal points for optimal luminosity gain. This will be discussed in more detail in a later subsection.

B. Beam focusing by tunneling ionization

As mentioned in the previous section, the major self-ionization process is tunneling ionization, while that due to collisional ionization has, at most, a small effect and, hence, can be neglected. The electric fields of electron and positron beams at SLC are strong enough to ionize a gas into a plasma through the mechanism of tunneling ionization. This mechanism of pinching the beams is attractive, since to form a plasma externally in the interaction region is nontrivial. It is important to determine from simulations whether this self-ionization mechanism is able to pinch the beams to achieve enough gain in luminosity for e^+e^- collisions in plasma lenses. As mentioned before, the maximum of the enhancement factor depends on the focusing strength and thickness of the plasma lens. By varying the gas density and lens thickness for fixed beam parameters, it is possible to determine design parameters for implementing a plasma lens in the final focusing region of SLC.

The criterion for the ionization of a gas element in our system of simulation is given by Eq. (17). For every grid point in our simulation mesh, the ionization rate function W is accumulated at every time step as the beams traverse the gas. The gas element is turned into a plasma element when the integral in Eq. (17) is greater than or

equal to 1. The gas will be ionized at a distance behind the beam fronts, which is determined by the beam parameters. Because of this, the beam fronts will never see the plasma and therefore will not be focused at all. Moreover the cores of the beams do not experience substantial focusing because the ionization begins at a radius of about 0.2σ and this degrades the final spot size and beam-beam disruption. Therefore, it is expected that the luminosity gain is less than that of colliding e^+e^- beams in a preformed plasma.

To study the propagation of electron and positron beams in gases, we choose the gas density and lens thickness to be $6 \times 10^{18} \text{ cm}^{-3}$ and 4.0 mm, respectively. These lens parameters correspond to maximum luminosity enhancement in a gas for the above beam parameters, the result obtained from simulations with varied gas densities and lens thicknesses (see the next subsection).

In Fig. 2, we show the simulation results for the behaviors of the e^+ and e^- beams as they traverse and collide in a gas of density $6 \times 10^{18} \text{ cm}^{-3}$. In this case, the beams are focused by the beam-ionized plasma. Initially there is no plasma and the gas fills the whole region of the figures. Again, the electrons are injected from the left boundary and the positrons from the right, and they are shown separately. The gas is subsequently ionized by the beams through tunneling ionization as described in Sec. III B. Thus the plasma profile depends on the properties of the beams. In particular, the gas starts to ionize into plasma at a certain distance behind the beam front. Fig-

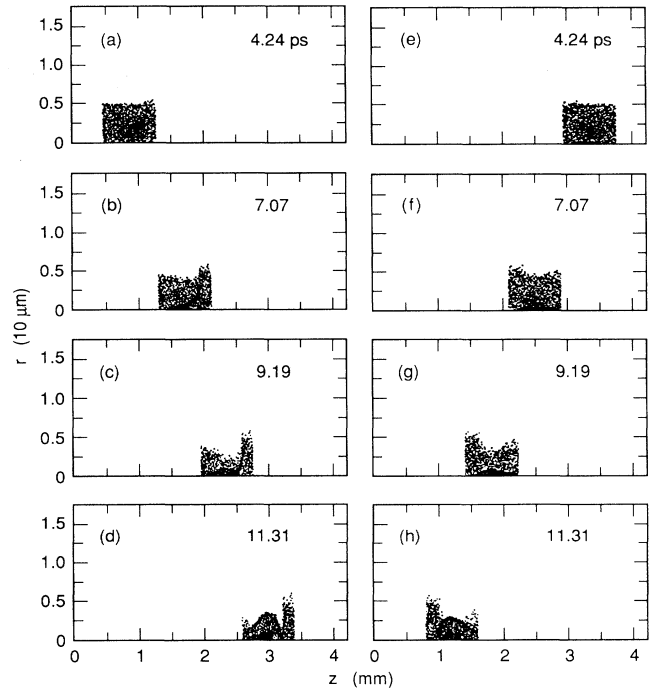


FIG. 2. Collision of e^+ and e^- beams in a beam-ionized plasma. (a)–(d) are four different snapshots at 4.24, 7.07, 9.19, and 11.31 psec for the e^- beam; (e)–(h) are for the corresponding e^+ beam.

ures 2(a)–2(d) and 2(e)–2(h) are snapshots at four different time steps for the distributions of the e^- and e^+ beams, respectively. The description of the focusing of the individual beams and their collision is similar to the case with a preformed plasma. The main difference is that a larger portion of the front part of the beams is not focused at all during the entire passage of the beams through the lens. The electric fields at the front are not strong enough to trigger tunneling ionization of the gas and therefore this part is not focused. Nevertheless, the rear portion of the beams experiences the response of the ionized plasma and will be focused [see Figs. 2(c)–2(d) and 2(g)–2(h)].

Figures 3(a) and 3(b) show the distributions of the plasma electrons and ions (protons) at time 7.07 psec after injection, respectively. This should be compared with the corresponding beam distributions at the same time step in Figs. 2(b) and 2(f). It can be seen that tunneling ionization takes place at a distance of about 0.2 mm behind the beam fronts. The first σ_z of the beams in this example is not focused (remember $\sigma_z = 0.2$ mm). Note also that the gas around the axis at the front parts of the beams is not ionized since the beam field diminishes to zero on the beam axis. The electric field in this region is not high enough to trigger tunneling ionization. This will degrade the focusing strength to a certain extent for those particles near the axis. Once the gas is ionized, the electrons and ions of the plasma will oscillate. The motion of the ions is not negligible and results in better focusing at the rear of the beams. This is clearly seen for the electron beam in Fig. 2(b), in which the front part and those particles near the axis are not focused, while the rear part is pinched much better (note the banana shape of the particles in the central region). Furthermore, it should be noted that the positron beam ionizes the gas further out from the axis than does the electron beam. This is because the screening of charges is more effective for the electron beam, resulting in a steeper decay of the electric field in the radial direction.

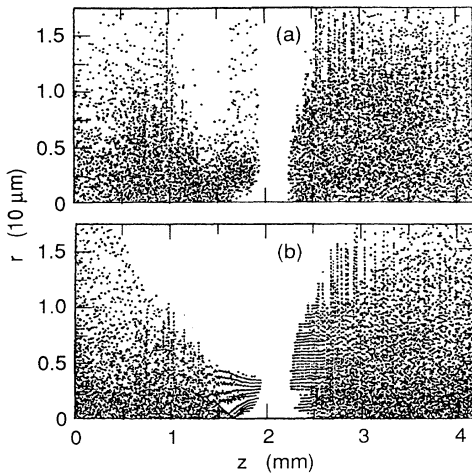


FIG. 3. Distributions of (a) ionized gas electrons and (b) ionized gas protons at a snapshot of 7.07 psec.

C. Luminosity enhancement at SLC

Having described the optics for the electron and positron beams, we next look into the physics of beam-beam interaction inside a plasma. The disruption due to mutual pinching between the colliding e^+e^- beams in a vacuum has been studied in detail [11,12]. In the situation where the e^+e^- beams collide inside a plasma, the mechanism is modified. When the beams overlap, the total beam current is increased; therefore we expect an increase of the “return current” induced in the plasma. The return current acts to reduce the magnetic focusing forces and the mutual beam-beam pinching. On the other hand, in the same beam overlapping region, the net space charge is reduced. Therefore, we expect a decrease of the space-charge perturbation in the plasma. This helps to reduce the influence of the plasma on the beam-beam disruption.

The overall enhancement of luminosity in our scheme can be estimated as

$$H_D = \frac{H_{D1}H_{D2}}{H_{D0}}, \quad (20)$$

where H_{D1} is the “geometric” enhancement due to the reduction of beam sizes by the plasma lens, and H_{D0} and H_{D2} are the disruption enhancement, due to beam-beam interaction with and without the plasma lens, respectively. Since the plasma-focused e^+ and e^- beams are different sizes, the “geometric” enhancement (excluding depth of focus and disruption effects) in luminosity is

$$H_{D1} = \frac{2\sigma_{r0}^{*2}}{\sigma_-^{*2} + \sigma_+^{*2}}. \quad (21)$$

We have shown that the mechanism of self-ionization of a gas can pinch a relativistic e^+ or e^- beam. To ensure that the two beams collide at the optimal position, we implemented a luminosity calculation in CONDOR to determine the thickness of the plasma lens. The focal length of the plasma lens is given by

$$s^* = \frac{\pi}{2\sqrt{K}}, \quad (22)$$

where $K = 2\pi r_e n_p / \gamma$ is the focusing strength of the lens determined by the plasma density n_p , and r_e is the classical electron radius. If the e^+ and e^- beams are focused evenly, the plasma lens thickness should be $l = 2s^*$. Because of various nonlinear effects, however, the desirable lens thickness cannot be determined analytically. We therefore rely on simulation to determine the optimal lens parameters. In CONDOR simulation, the focal length is determined by optimizing the longitudinal length of the plasma for maximum gain in luminosity.

The luminosity for e^+e^- collisions is defined as the four-dimensional phase-space integral

$$\mathcal{L} = f \int n_1(x, y, z, t) n_2(x, y, z', t) dx dy dz dt, \quad (23)$$

where $z' = z - ct$, n_1 and n_2 are the densities of electrons and positrons, respectively, as functions of time, and f is the repetition rate of collisions. When e^+ and e^- beams

collide in a vacuum, luminosity will be enhanced by disruption caused by the bending of particle trajectories by the electromagnetic fields of the oncoming beam. To quantify this luminosity enhancement, we define the enhancement factor

$$H_{D0} = \frac{\mathcal{L}}{\mathcal{L}_0}, \quad (24)$$

where $\mathcal{L}_0 = fN^2/4\pi\sigma_r^2$ is the nominal luminosity. When e^+ and e^- beams collide in plasma, the luminosity is further enhanced by plasma focusing.

In Fig. 4, we show the dependence of the luminosity enhancement factor H_D as a function of the plasma lens thickness L for various gas densities. The numbers of particles in the beams are 4×10^{10} and 3×10^{10} , respectively, for the two sets of curves. We have chosen these different beam currents to illustrate the effects of beam properties on tunneling ionization. Note also that 3×10^{10} is the present SLC operating current. We do not distinguish the underdense and overdense regimes, and vary the gas density to obtain the maximal luminosity gain. The gas density varies from 2×10^{18} to $6 \times 10^{18} \text{ cm}^{-3}$. Let us first consider the case where $N = 4 \times 10^{10}$. We see that for a gas density of 6×10^{18} , we achieve the maximum gain in luminosity, mainly because of the stronger focusing strength produced by a higher density gas. The optimal lens thickness is found to be about 4.0 mm and this is in good agreement with the theoretical estimate from Eq. (6). It is also seen that the enhancement factor does not change sensitively around this optimal lens thickness. This shows that the enhancement is not very sensitive to the lens thickness or to the longitudinal offset of the two beams. For $N = 3 \times 10^{10}$, because the beam fields are weaker, and the corresponding focusing strength is not as strong as for $N = 4 \times 10^{10}$, a longer lens thickness (5.0 mm) is required to achieve the maximum gain in luminosity, and the optimal gain in luminosity is smaller than that for $N = 4 \times 10^{10}$. This is expected because the electric field is weaker for lower current, and hence the ionization probability will decrease.

In the preceding subsection, we saw that the electrons are focused somewhat better than the positrons. It would be better to have the beams focused with a longitudinal offset that allows the beams to meet when they have the smallest spot sizes. However, from our simulation, an offset of about 0.67 psec with the positron beam injected later only increase the luminosity gain by a few percent. This is again an illustration of the relatively flat behavior of the distributions near the optimal lens thickness. Furthermore, increasing the gas density beyond $6 \times 10^{18} \text{ cm}^{-3}$ does not further increase the luminosity gain. This is expected. As in the overdense regime, the focusing will basically be determined by the beam parameters, and the aberration effects will increase the spot sizes at the interaction point for higher density gases.

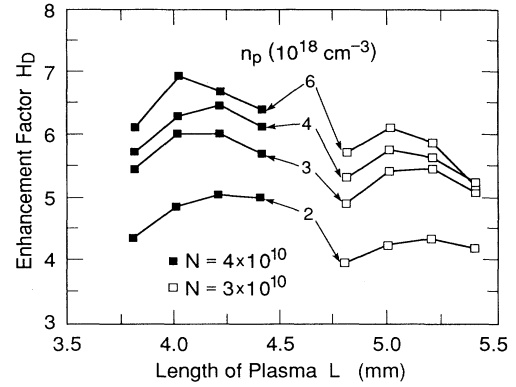


FIG. 4. Luminosity enhancement factor as a function of plasma lens thickness for different plasma densities n_p . The beam currents are taken to be 3×10^{10} and 4×10^{10} for the two sets of curves.

V. CONCLUSIONS

We have used the particle-in-cell code CONDOR to study beam-plasma interactions and have demonstrated the focusing of relativistic beams in plasmas. By focusing the colliding e^- and e^+ beams in plasmas, the luminosity in high-energy linear collider experiments can be enhanced as a consequence of the self-focusing of the beams.

We have also shown that considerable luminosity enhancement can be obtained by the process of tunneling ionization. A luminosity enhancement factor of 5 to 7 can be achieved by this process for SLC beam parameters of $N = 3 \times 10^{10}$ and $N = 4 \times 10^{10}$, $\sigma_r = 2 \text{ } \mu\text{m}$, $\sigma_z = 0.2 \text{ mm}$, and an emittance of $4 \times 10^{-10} \text{ mrad}$. For a repetition rate of 120 sec^{-1} , it will enhance the luminosity to $\sim 3 \times 10^{30} \text{ cm}^{-1} \text{ sec}^{-1}$ at SLC. It should be noted that further luminosity enhancement is possible, especially in the core regions, by way of collisional ionization, which we have neglected in this analysis. The complementary roles of impact ionization and tunneling ionization will play a more important role in the Next Linear Collider (NLC). For example, for NLC beams with $N = 0.65 \times 10^{10}$, $\sigma_x = 300 \text{ nm}$, and $\sigma_y = 3 \text{ nm}$, impact ionization will be saturated. This must be taken into account in luminosity calculations.

ACKNOWLEDGMENTS

We are grateful to M. Briedenbach of SLD for earlier discussions which triggered the investigation of beam self-ionization. We also thank K. Bane, S. Brandon, K. Eppley, and K. Ko for useful discussions. P.C. and C.-K.N. were supported by Department of Energy Contract No. DE-AC03-76SF00515. S.R. was supported by Department of Energy Contract No. DE-AS03-88ER40381.

- [1] P. Chen, *Part. Accel.* **17**, 121 (1987).
- [2] J. B. Rosenzweig *et al.*, *Phys. Fluids B* **2**, 1376 (1990).
- [3] H. Nakanishi *et al.*, *Phys. Rev. Lett.* **66**, 1870 (1990).
- [4] J. B. Rosenzweig and P. Chen, *Phys. Rev. D* **39**, 2039 (1989).
- [5] P. Chen, S. Rajagopalan, and J. B. Rosenzweig, *Phys. Rev. D* **40**, 923 (1989).
- [6] J. J. Su, T. Katsouleas, J. M. Dawson, and R. Fidele, *Phys. Rev. A* **41**, 3321 (1990).
- [7] P. Chen, *Phys. Rev. A* **39**, 45 (1992).
- [8] B. Aiminetti, S. Brandon, K. Dyer, J. Moura, and D. Nielsen, Jr., *CONDOR User's Guide, Livermore Computing Systems Document* (Lawrence Livermore National Laboratory, Livermore, CA, 1988).
- [9] F. LeDiberder (private communication).
- [10] L. D. Landau and E. M. Lifshitz, *Quantum Mechanics: Non-Relativistic Theory*, 3rd ed. (Pergamon, New York, 1981), p. 293.
- [11] R. Hollebeek, *Nucl. Instrum. Methods* **184**, 333 (1981).
- [12] P. Chen and K. Yokoya, *Phys. Rev. D* **38**, 987 (1988).